Inorg. Chem. **2008**, *47*, 2083−2088

Mechanistic Aspects of the Reaction of Th^+ and Th^{2+} with Water in the Gas Phase

Gloria Mazzone, Maria del Carmen Michelini, Nino Russo,* and Emilia Sicilia

Dipartimento di Chimica and Centro di Calcolo ad Alte Prestazioni per Elaborazioni Parallele e Distribuite-Centro d'Eccellenza MURST, Università della Calabria, I-87030 Arcavacata di Rende, Italy

Received September 12, 2007

Density functional theory calculations were performed to study the gas-phase reaction of Th^+ and Th^{2+} with water. An in-depth analysis of the reaction pathways leading to different reaction products is presented. The obtained results are compared to experimental data and to the previously studied reactions of U cations with water.

1. Introduction

In the last decades, reactions of single- and double-charged actinide cations with small molecules have been a subject of considerable interest.[1–6] One of the fundamental goals of those investigations has been to analyze their distinctive electronic structures and chemical properties without interference by bulk effects that are present in condensed systems. Particularly interesting is the analysis of the potential 5f electron contribution to reactivity. It is known that in contrast to the corelike 4f electrons, which do not participate in bond formation, for early actinides the 5f electrons are relatively high in energy and spatially extended. In the case of lanthanide cations, it has been pointed out that at least two non-f electron configurations are required in order to activate alkanes.[7] Further, it has been found that the efficiency of activation of hydrocarbons by Ln^+ in the gas phase correlates with the promotion energy from the ground-state electronic configuration to the lowest-lying [Xe] $4f^{n-2}5d^16s^1$ configuration.[7] In the case of actinides, a direct participation of the 5f electrons in the bonding might allow certain reactions to proceed without promotion to outer 6d or 7s orbitals.

Experimentally (Fourier transform ion cyclotron resonance mass spectrometry, FTICR-MS),[2–4] the following reaction products were detected during the reaction of Th^+ and Th^{2+} with water:

$$Th^{+(2+)} + H_2O \rightarrow ThO^{+(2+)} + H_2 \quad (1)$$

$$Th^{+(2+)} + H_2O \rightarrow ThOH^{+(2+)} + H \quad (2)$$

In the case of Th^+, the main product is the monoxide, with a substantial fraction of $ThOH^+$ (branching ratio 35%).[2,4] For Th^{2+}, FTICR-MS studies[3] on the product distribution indicate the formation of the hydroxyl as the primary product channel, with a branching ratio of 90%. We note that it was previously assumed that the $ThOH^{+(2+)}$ connectivities were that of the hydroxyl; however, our results indicate that, in the case of the monopositive structure, the oxide hydride, $HThO^+$, is the energetically favored isomer. Hereafter, we will refer to the hydroxyl structures by $ThOH^{+(2+)}$ and to the oxide hydride isomers by $HThO^{+(2+)}$.

The main goal of this work is to give insight into the mechanistic aspects of the reaction of Th^+ and Th^{2+} with water, comparing the obtained results with the existent experimental data[2–4] as well as with the previously studied $U^{+(2+)} + H_2O$ reactions.[5]

2. Computational Details

On the basis of the performance observed in our previous studies of the reaction of U cations with water,[5,6] two different approaches of density functional theory (DFT) were used to perform this study.

* To whom correspondence should be addressed. E-mail: nrusso@unical.it.

(1) (a) Gibson, J. K.; Marçalo, J. *Coord. Chem. Rev.* **2006**, *250*, 776. (b) Gibson, J. K. *Int. J. Mass Spectrom.* **2002**, *214*, 1. (c) Jackson, G. P.; King, F. L.; Goeringer, D. E.; Duckworth, D. C. *J. Phys. Chem. A* **2002**, *106*, 7788. Correction: *J. Phys. Chem. A***2004**, *108*, 2139. (d) Santos, M.; Marçalo, J.; Leal, J. P.; Pires de Matos, A.; Gibson, J. K.; Haire, R. G. *Int. J. Mass Spectrom.* **2003**, *228*, 457.

(2) Santos, M.; Marçalo, J.; Pires de Matos, A.; Gibson, J. K.; Haire, R. G. *J. Phys. Chem. A* **2002**, *106*, 7190.

(3) Gibson, J. K.; Haire, R. G.; Santos, M.; Marçalo, J.; Pires de Matos, A. *J. Phys. Chem. A* **2005**, *109*, 2768.

(4) Cornehl, H. H.; Wesendrup, R.; Diefenbach, M.; Schwarz, H. *Chem.—Eur. J.* **1997**, *3*, 1083.

(5) Michelini, M. C.; Russo, N.; Sicilia, E. *Angew. Chem., Int. Ed.* **2006**, *45*, 1095.

(6) Michelini, M. C.; Russo, N.; Sicilia, E. *J. Am. Chem. Soc.* **2007**, *129*, 4229.

(7) (a) Schilling, J. B.; Beauchamps, J. L. *J. Am. Chem. Soc.* **1988**, *110*, 15. (b) Cornehl, H. H.; Heinemann, C.; Schroeder, D.; Schwarz, H. *Organometallics* **1995**, *14*, 992.

10.1021/ic701789n CCC: $40.75
Published on Web 02/15/2008

First, the zero-order regular approximation was used together with the PW91 functionals (exchange and correlation)[8] and the TZ2P (TZP for Th) basis set as implemented in the ADF package[9] (we refer to these results as PW91/ZORA hereafter). Second, the B3LYP[10] hybrid functional was used together with the Stuttgart relativistic effective core potential (small core).[11] The 6-311++G(d,p) basis set of Pople and co-workers was employed for O and H atoms (B3LYP/SDD; SDD = Stuttgart relativistic effective core potential).[12] Similar levels of theory were successfully employed for a series of studies on the reactivity of transition-metal cations with small ligands.[13] The B3LYP/SDD calculations were carried out using the *Gaussian03* package.[14] Single-point CCSD(T) calculations on the B3LYP-optimized structures were carried out using the same basis set [CCSD(T)//B3LYP]. We have examined the T1 diagnostic proposed by Lee and Taylor,[15] which has shown to be a reliable measure of the importance of nondynamical electron correlation and an indicator as to whether it is appropriate to use a single-reference-based electron correlation procedure. The threshold of 0.02 is usually accepted to support the validity of a monodeterminantal description of the reference wave function. Of all of the species studied here, only three structures have T1 values greater than 0.02, namely, the first minimum (T1 = 0.033) and the TS1 (T1 = 0.040) on the doublet spin $Th^+ + H_2O$ surface and the triplet-state TS1 (T1 = 0.027) of the $Th^{2+} + H_2O$ reaction. The rest of the structures have T1 values lying between 0.013 and 0.019.

Computations of open-shell systems were performed using spin-unrestricted methods. No spin contamination problems were found, with the only exception being two doublet spin species: Th^+-OH_2 and TS1 (at both levels of theory). At the B3LYP/SDD level, the problem was solved after annihilation of the first spin contaminant because $\langle S2\rangle_A$ values never exceded 0.76. We note that these are the species that have the largest T1 values.

Table 1. First and Second Adiabatic Ionization Energies (IE1 and IE2, in eV) for Th and ThO

	Th		ThO	
method	IE1	IE2	IE1	IE2
PW91/ZORA	5.2	12.2	6.4	12.2
B3LYP/SDD	5.9	11.7	6.3	11.8
expt	6.3[a]	11.9[b]	6.6[a]	≤12.8[c]

[a] Precise values: 50868.71(8) and 53253.8(2) cm^{-1}, respectively.[20] [b] Meggers, W. F.; Corliss, C. H.; Scribner, B. F. *Natl. Bur. Stand. (U.S.), Monogr. 145* (1975), taken from http://physics.nist.gov/PhysRefData/. [c] Reference 3.

Table 2. Experimental and Calculated BDEs (in kJ/mol) of ThO^+ ($^2\Sigma$) and ThO^{2+} ($^1\Sigma_g$)[a]

method	BDE ThO^+ ($^2\Sigma$)[b]	BDE ThO^{2+} ($^1\Sigma_g$)[b]
PW91/ZORA	997 (1.820)	993 (1.783)
B3LYP/SDD	846 (1.808)	833 (1.771)
expt	866 ± 21[c] (1.807)[d]	≥751[e]

[a] Th−O bond lengths (in Å) are given in parentheses. [b] BDE calculated for the following dissociation processes (all of the species in their ground states): $ThO^{+(2+)} \rightarrow Th^{+(2+)} + O$. [c] Data taken from ref 1a. [d] Reference 20. [e] Reference 3.

We have also checked the stability of restricted closed-shell species (singlet-state structures) at the B3LYP/SDD level. To our knowledge, it is not possible to perform this type of correction with the ADF package.

Spin–orbit effects were not treated explicitly in this work.

All of the structures were fully optimized, and the nature of the stationary points was characterized by a vibrational analysis performed within the harmonic approximation. The zero-point vibrational energy corrections were included in all of the reported relative energies. We have ensured that every transition state has only one imaginary frequency. Intrinsic reaction coordinate calculations were performed to confirm that the transition states connect reactants and products.

For both studied reactions, two different spin states were considered: the ground and lowest-lying excited spin states of the bare cations. Therefore, we have studied quartet and doublet spin states for $Th^+ + H_2O$ and triplet and singlet states in the case of the Th^{2+} reaction.

Natural bond orbital (NBO) analysis[16] was performed for all of the reaction products with the aim of gaining insight into their bonding properties.

3. Results and Discussion

3.1. Preliminary Calculations. Preliminary calculations of the first and second ionization energies of the bare thorium and thorium monoxide and of the bond dissociation energies (BDEs) of the cationic thorium monoxides (ThO^+ and ThO^{2+}) show that the computational approaches used here give results that are in reasonable agreement with the experimental data (Tables 1 and 2).

The ground state of Th^+ is a ^4F derived from the [Rn] $6d^27s^1$ electronic configuration, whereas Th^{2+} has a ^3H ([Rn] 6d5f) ground-state configuration.[17] At the PW91/ZORA level, we correctly identify the ground-state electronic configuration of Th^+, whereas at the B3LYP/SDD level, we have found some discrepancies because the doublet [Rn]

(8) (a) Burke, K.; Perdew, J. P.; Wang Y. In *Electronic Density Functional Theory: Recent Progress and New Directions*; Dobson, H. F., Vignale, G., Das, M. P., Eds.; Plenum: New York, 1998. (b) Perdew, J. P. In *Electronic Structure of Solid '91*; Ziesche, P., Eschrig, H., Eds.; Akademie Verlag: Berlin, 1991; p 11. (c) Perdew, J. P.; Burke, K.; Wang, Y. *Phys. Rev. B* **1996**, *54*, 16533. (d) Perdew, J. P.; Chevary, J. A.; Vosko, S. A.; Jackson, K. A.; Pederson, M. R.; Singh, D. J.; Fiolhais, C. *Phys. Rev. B* **1992**, *46*, 6671. (e) Perdew, J. P.; Chevary, J. A.; Vosko, S. H.; Jackson, K. A.; Pederson, M. R.; Singh, D. J.; Fiolhais, C. *Phys. Rev. B* **1993**, *48*, 4978.

(9) (a) te Velde, G.; Bickelhaupt, F. M.; van Gisbergen, S. J. A.; Fonseca Guerra, C.; Baerends, E. J.; Snijders, J. G.; Ziegler, T. *J. Comput. Chem.* **2001**, *22*, 931. (b) Fonseca Guerra, C.; Snijders, J. G.; te Velde, G.; Baerends, E. J. *Theor. Chem. Acc.* **1998**, *99*, 391. (c) ADF2004.01, SCM, Theoretical Chemistry, Vrije Universiteit, Amsterdam, The Netherlands, http://www.scm.com..

(10) (a) Becke, A. D. *J. Chem. Phys.* **1993**, *98*, 5648. (b) Lee, C.; Yang, W.; Parr, R. G. *Phys. Rev. B* **1988**, *37*, 785.

(11) (a) http://www.theochem.unistuttgart.de/pseudopotentiale/. (b) Küchle, W.; Dolg, M.; Stoll, H.; Preuss, H. *J. Chem. Phys.* **1994**, *100*, 7535.

(12) (a) Krishnan, R.; Binkley, J. S.; Seeger, R.; Pople, J. A. *J. Chem. Phys.* **1980**, *72*, 650. (b) Blaudeau, J.-P.; McGrath, M. P.; Curtiss, L. A.; Radom, L. *J. Chem. Phys.* **1997**, *107*, 5016. (c) Clark, T.; Chandrasekhar, J.; Schleyer, P. v. R. *J. Chem. Phys.* **1983**, *74*, 294.

(13) (a) For instance, See: Michelini, M. C.; Russo, N.; Sicilia, E. *J. Phys.Chem. A* **2002**, *106*, 8937. (b) Chiodo, S.; Kondakova, O.; Michelini, M. C.; Russo, N.; Sicilia, E. *Inorg. Chem.* **2003**, *42*, 8773. (c) Chiodo, S.; Kondakova, O.; Michelini, M. C.; Russo, N.; Sicilia, E. *J. Phys. Chem. A* **2004**, *108*, 1069. (d) Michelini, M. C.; Russo, N.; Alikhani, M. E.; Silvi, B. *J. Comput. Chem.* **2004**, *25*, 1647. (e) Michelini, M. C.; Russo, N.; Sicilia, E. *Inorg. Chem.* **2004**, *43*, 4944. (f) Michelini, M. C.; Russo, N.; Alikhani, M. E.; Silvi, B. *J. Comput. Chem.* **2005**, *26*, 1284. (g) Martinez, M.; Rivalta, I.; Michelini, M. C.; Russo, N.; Sicilia, E. *Inorg. Chem.* **2005**, *44*, 4944.

(14) Frisch, M. J.; *Gaussian 03*; see the Supporting Information for the full citation.

(15) (a) Lee, T. J.; Taylor, P. R. *Int. J. Quantum Chem., Quantum Chem. Symp.* **1989**, *23*, 199. (b) Lee, T. J.; Rice, J. E.; Scuseria, G. E.; Schaefer, H. F. *Theor. Chim. Acta* **1989**, *75*, 81.

(16) (a) Reed, A. E.; Weinhold, F. *J. Chem. Phys.* **1985**, *83*, 1736. (b) Reed, A. E.; Curtiss, L. A.; Weinhold, F. *Chem. Rev.* **1988**, *88*, 899.

(17) Blaise, J.; Wyart, J.-F. International Tables of Selected Constants, Energy Levels and Atomic Spectra of Actinides, Vol. 20, Tables of Constants and Numerical Data, Paris, 1992, taken from http://www.lac.u-psud.fr/Database/Contents.html.

Table 3. Relative Energies (in kJ/mol) of the Th^+ and Th^{2+} Ground and Excited States[a]

Th^+	expt[b]	PW91/ZORA	B3LYP/SDD
[Rn] $6d^27s$ (4)	0.00	0	24
[Rn] $6d7s^2$ (2)	22.25	46	31
[Rn] $5f7s^2$ (2)	53.71	17	0
[Rn] 5f6d7s (4)	75.22	40	57
[Rn] $6d^3$ (4)	83.76	69	97

Th^{2+}	expt[b]	PW91/ZORA	B3LYP/SDD
[Rn] 5f6d (3)	0.00	21	20
[Rn] $6d^2$ (3)	0.37	48	59
[Rn] 5f7s (3)	30.08	0	0
[Rn] 6d7s (3)	65.70	72	90
[Rn] $7s^2$ (1)	142.70	174	171
[Rn] $5f^2$ (3)	180.83	120	123

[a] Spin multiplicities are given in parentheses. [b] Statistically averaged spin–orbit energy levels. Energy levels are taken from ref 17.

$5f7s^2$ configuration is the lowest-energy configuration, with the quartet [Rn] $6d^27s$ around 24 kJ/mol higher in energy. For Th^{2+}, both studied levels of theory have indicated the triplet [Rn] 5f7s configuration as the ground state, whereas the triplet [Rn] 5f6d lies 20 kJ/mol higher in energy. The calculated relative energies of the lowest-lying excited states with respect to the cation ground states are collected in Table 3. We note that, because we have not performed spin–orbit calculations, our results correspond to the average of the various experimental spin–orbit levels. For this reason and with the aim of performing a more realistic comparison, we perfomed a statistical average of the energy of the experimental spin–orbit levels, which were taken from ref 17.

The incorrect prediction of the ordering of the states illustrates one of the major shortcomings of the DFT approach, which has been largely discussed in the case of transition metals.[13c,18] We consider, however, that in the present case the error associated with the incorrect assignment of the cation ground states does not have a strong influence on the shape of the potential energy profiles, because, as we will show in the next section, the low-spin states are strongly stabilized along the reaction pathways. We note that in the present case CCSD(T)/SDD calculations do not improve the energy gaps obtained at the DFT level. In the case of Th^+, the errors obtained at that level are similar to those obtained at B3LYP/SDD, whereas in the case of Th^{2+}, the performance is worse than that observed for DFT calculations. For that reason, we only report CCSD(T)// B3LYP barrier heights, which in our opinion can be considered reliable, as well as the obtained T1 values.

3.2. Reaction Mechanisms. According to our calculations, the reactions of Th^+ and Th^{2+} with water have similar mechanisms, which can be outlined as follows. Starting from the reactants, the potential surface is strongly attractive in nature and leads to a deep potential minimum in which the metal cation and the water molecule form a very stable association complex, $Th^{+(2+)}-OH_2$. After rising to the first transition state (TS1) energy, which occurs *below* the energy of the reactants, a hydrogen atom is shifted from oxygen to the metal atom, leading to a hydrido−metal−hydroxy, $HThOH^{+(2+)}$, insertion intermediate. Then, the reaction proceeds toward the formation of the dehydrogenation products, reaction (1), through a concerted four-center elimination of H_2, or the formation of $ThOH^{+(2+)}$, reaction (2), as a result of a simple cleavage of the Th−H bond in the insertion intermediate. The possible formation of $HThO^{+(2+)}$ isomers by cleavage of the O−H bond was also considered. In the case of the dipositive cation, we have also analyzed the charge-separation asymptotes, namely, the formation of $ThOH^+$ and $HThO^+$ ($+H^+$).

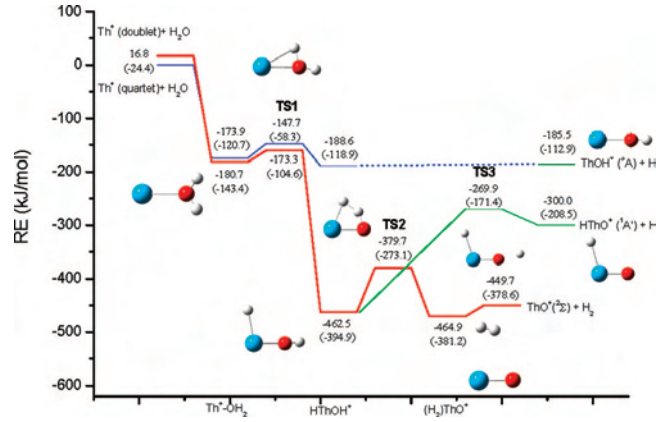

Figure 1. Potential energy profiles for the reaction of $Th^+ + H_2O$ at the PW91/ZORA (B3LYP/SDD) level of theory, corresponding to the quartet and doublet spin states.

The dehydrogenation pathway involves the formation of a second insertion intermediate, $(H_2)ThO^{+(2+)}$, just after the system surpasses the second transition state (TS2). We have also taken into account the possible formation of the dihydride thorium oxo, the $(H)_2ThO^{+(2+)}$ isomer, which was found to be an important species in the case of the neutral $Th + H_2O$ reaction.[19] Our calculations indicate that, in the case of the cationic species, these structures are higher-energy isomers that are not involved in the dehydrogenation paths.

The overall potential energy profile for the reaction of $Th^+ + H_2O$ is sketched in Figure 1, whereas that of $Th^{2+} + H_2O$ is shown in Figure 2. The most relevant geometrical parameters of all of the involved stationary points at their lowest-energy spin states are collected in Figures 3 and 4, respectively.

For $Th^+ + H_2O$, the reaction path evolves along the doublet spin surface from the formation of the Th^+-OH_2 initial complex, whereas in the case of Th^{2+}, the reaction starts at the triplet reactant ground state, and only after the system overcomes the first transition state does an intersystem crossing to the singlet spin state take place. The rest of the reaction evolves along the singlet spin surface.

For $Th^+ + H_2O$, the dehydrogenation process shows an exothermicity of almost 450 kJ/mol at the PW91/ZORA (379 kJ/mol at the B3LYP/SDD). From experimental BDE data, the formation of ThO^+ concomitantly with the loss of H_2 is

(18) (a) Ricca, A.; Bauschlicher, C. W., Jr. *Theor. Chim. Acta* **1995**, *92*, 123. (b) Holthausen, M. C.; Fiedler, A.; Schwarz, H.; Koch, W. *J. Phys. Chem.* **1996**, *100*, 6236. (c) Ricca, A.; Bauschlicher, C. W., Jr. *J. Phys. Chem.* **1995**, *99*, 9003. (d) Filatov, S.; Shaik, S. *J. Phys. Chem. A* **1998**, *102*, 3835.

(19) Liang, B.; Andrews, L.; Li, J.; Bursten, B. E. *J. Am. Chem. Soc.* **2002**, *124*, 6723.

(20) Goncharov, V.; Heaven, M. C. *J. Chem. Phys.* **2006**, *124*, 064312.

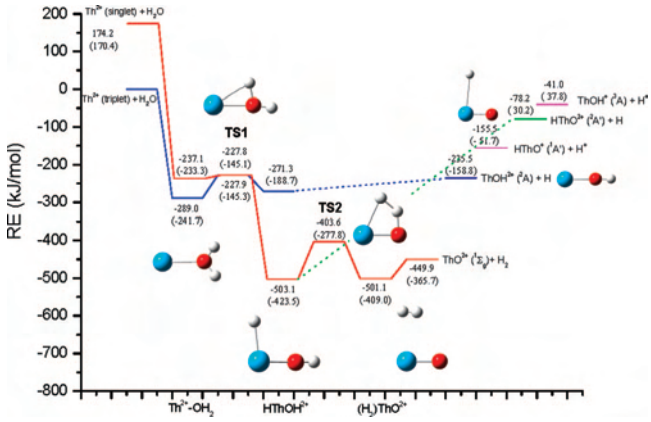

Figure 2. Potential energy profiles for the reaction of $Th^{2+} + H_2O$ at the PW91/ZORA (B3LYP/SDD) level of theory, corresponding to the singlet and triplet spin states.

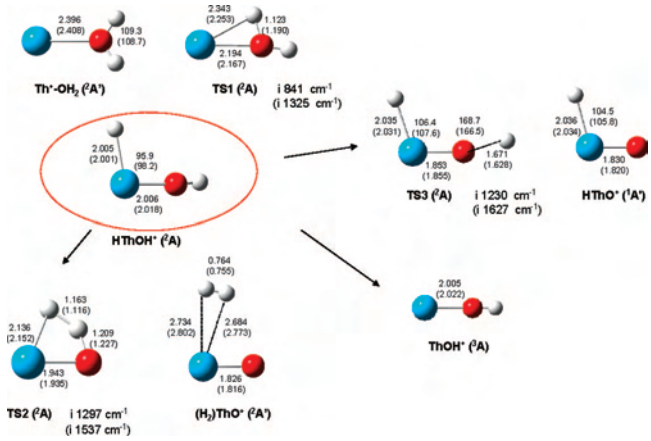

Figure 3. Geometrical parameters of all of the minima and transition states (lowest-energy spin state species) involved in the reaction of Th^+ with H_2O, at the PW91/ZORA (B3LYP/SDD) level of theory. Bond lengths are in angstroms, and angles are in degrees.

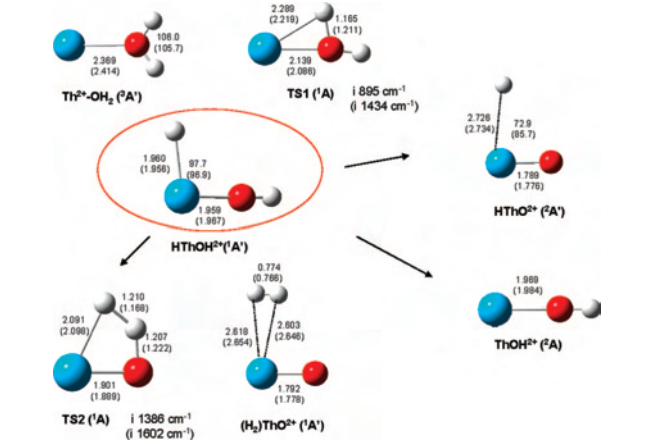

Figure 4. Geometrical parameters of all of the minima and transition states (lowest-energy spin state species) involved in the reaction of Th^{2+} with H_2O, at the PW91/ZORA (B3LYP/SDD) level of theory. Bond lengths are in angstroms, and angles are in degrees.

expected to be exothermic by 374.5 kJ/mol. The calculated exothermicity for the dicationic reaction is comparable to that of $Th^+ + H_2O$ (Figure 2). This is not surprising considering that the computed BDEs of $ThO^+(^2\Sigma)$ and ThO^{2+} ($^1\Sigma_g$) are very close, at both levels of theory (Table 2).

Table 4. Activation Barriers (in kJ/mol) of the Transition States

Th^+-H_2O	PW91/ZORA (B3LYP/SDD) [CCSD(T)//B3LYP]	U^+-H_2O	PW91/ZORA[a] (B3LYP/SDD)
TS1[b]	7.4 (38.7) [75.1]	TS1	17.9 (60.8)
TS2[c]	82.8 (121.3) [128.3]	TS2	66.1 (132.1)
dissociation barrier[d]	15.2 (3.1) [7.9]	dissociation barrier	47.7 (73.0)

$Th^{2+}-H_2O$	PW91/ZORA (B3LYP/SDD) [CCSD(T)//B3LYP]	$U^{2+}-H_2O$	PW91/ZORA[a] (B3LYP/SDD)
TS1[b]	61.1 (96.6) [114.3]	TS1	112.8 (143.4)
TS2[c]	99.5 (145.5) [151.8]	TS2	108.2 (124.7)
dissociation barrier[d]	51.2 (43.2) [50.2]	dissociation barrier	86.1 (55.6)

[a] Reference 5. [b] Calculated as the energetic difference between the first transition state (TS1) and the initial complex ($Th^{+(2+)}-OH_2$), in their ground states. [c] Calculated as the energetic difference between the second transition state (TS2) and the first insertion intermediate ($HThOH^{+(2+)}$), in their ground states. [d] Energy difference between the dissociated products ($ThO^+ + H_2$ or $ThO^{2+} + H_2$) and the last intermediate $(H_2)ThO^{+(2+)}$.

Table 4 summarizes the activation barriers associated to all the transition states. With the aim of comparison we have also included the same data for the previously studied $U^{+(2+)} + H_2O$ reactions.[5]

In all cases, the transition states are well below the dissociation limit represented by the reactants. For both reactions, the second transition state involves the largest intrinsic energy barrier. We must mention that the very low TS1 energy barrier obtained at the PW91/ZORA level for the $Th^+ + H_2O$ reaction is associated with both doublet state species (Th^+-OH_2 and TS1) that have the largest T1 values and spin contamination problems. In fact, it is also the only case in which we have found a large difference between the barrier heights calculated at the CCSD(T)//B3LYP level with respect to those obtained at the DFT level. The very low energy involved in the H_2 elimination process ($Th^+ + H_2O$ reaction) is probably a consequence of repulsive effects between the unpaired electron localized on the metal atom and the H_2 molecule, which is already formed in the last $(H_2)ThO^+$ intermediate.

The calculated reaction barriers associated to the dehydrogenation process in the Th^{2+} reaction were found to be notably higher for the first transition state, as well as for the dissociation process. The TS2 barrier can be considered comparable in both reactions.

3.3. Reaction Products: Structural Properties and Bond Analysis. According to the NBO analysis, the Th−O bond in both cationic oxides can be described as a triple bond, which is formed mainly from almost pure O p orbitals and d−f hybrids of Th. For both monoxides, the metal hybrid orbitals have between 40 and 50% of f character and between 50 and 60% of d character (see Table S.1 of the Supporting Information). The description of the bond obtained at the present level of theory involves, therefore, an important participation of 5f orbitals. The polarization coefficients (e.g., 0.9 for O and 0.4 for Th) indicate that the Th−O bond can be considered as a highly polarized covalent bond. Both cationic oxides have an s-type lone pair on the O atom and, in the case of ThO^+ ($^2\Sigma$), there is also an unpaired electron

(s-type) localized on the metal atom. The NBO analysis indicates, therefore, that the bonding characteristics of both cations are very similar, supporting the comparable, very high BDEs. We have included a detailed description of the NBO analysis in Table S.1 of the Supporting Information.

The formation of the hydrido monoxide isomer, HThO, is highly favored only in the case of $HThO^+$ (singlet spin ground state). We note that the $ThOH^+$ isomer has a triplet spin ground state, with two unpaired electrons of s and d character localized on the metal atom. The NBO analysis predicts that this moiety is better described as formed from two units; namely, there is not a covalent bond between the metal atom and the O−H ligand. The NBO second-order perturbation analysis indicates that hyperconjugation between oxygen lone pairs and the vacant valence metal orbitals plays a role in stabilizing the structure. The natural population analysis (NPA) charge on the metal atom is +1.75e, notably lower than the corresponding value for the $HThO^+(^1A')$ isomer (+2.83 e) (Tables S.2 and S.3 of the Supporting Information). We note that the $HThO^+$ ($^1A'$) structure is the only of the $ThOH^{+(2+)}$ isomers that contains the Th cation at the formal oxidation state IV. The reason for which the $HThO^+$ isomer is energetically favored can also be understood by considering its formation from $ThO^+(^2\Sigma)$. The doublet ThO^+ ground state has an unpaired electron of s character localized on the metal atom. In $HThO^+$ ($^1A'$), the Th−H bond is formed from the unpaired Th electron, and the structure conserves the strong Th−O triple bond (Table S.1 of the Supporting Information). The bond distances clearly confirm this fact. The Th−O bond lengths are 2.005 and 1.820 Å in $ThOH^+$ (^3A) and $HThO^+$ ($^1A'$), respectively, at the PW91/ZORA level (Figure 3). The formation of $HThO^+$ ($^1A'$) could take place from the $HThOH^+(^2A)$ intermediate by cleaveage of the O−H bond. We have analyzed that process and found that it involves an intrinsic transition barrier height of around 200 kJ/mol (TS3 in Figures 1 and 3). We were unable to localize that transition state in the case of the dipositive reaction, and the *scan* calculations performed varying the H−Th bond length indicate that the metal−hydrogen bond breaking process is barrierless.

The $HThO^{2+}$ and $ThOH^{2+}$ isomers have doublet spin ground states, and the NPA charges borne by the cation are quite similar, +2.70 and +3.03e, respectively. The NBO analysis indicates that, as in the case of the monopositive structure, the $ThOH^{2+}$ (^2A) hydroxide is better described as formed from two fragments (Tables S.2 and S.3 of the Supporting Information). The metal unpaired electron has a mixed s−d−f character. The NBO description of the $HThO^{2+}$ ($^2A'$) structure indicates that the system is formed also from two fragments, the ThO^{2+} monoxide and an H atom. The unpaired electron is located on the 1s orbital of the H atom, the Th−O bond is very close to that of ThO^{2+} ($^1\Sigma_g$), and the Th−H distance is quite long, namely, 2.726 Å at the PW91/ZORA level (Figure 4).

The formation of $ThOH^{+(2+)}$ + H could happen directly from the high-spin $HThOH^{+(2+)}$ intermediates, which are energetically quite close to TS1 and have geometrical structures that are already prepared for that detachment (the H−Th bond lengths are 2.799 and 2.797 Å in $HThOH^+(^4A)$ and $HThOH^{2+}$ ($^3A''$), respectively, at the PW91/ZORA level). From the $HThOH^{+(2+)}$ intermediates (ground or excited states), the hydrogen-metal detachment process is barrierless, as confirmed by Th−H bond *scan* calculations.

3.4. Comparison with the $U^{+(2+)} + H_2O$ Reactions. The reaction mechanism for the activation of the O−H bond was studied according to a general scheme that involves the formation of an insertion intermediate $HMOH^{+(2+)}$ (M = U, Th), which is very often the key step of the process. The insertion intermediate is formed by the coupling of the unpaired electrons on the H and OH ligands with two metal atom valence electrons, which usually provokes a crossing between spin surfaces due to the stabilization of low spin states. In fact, for U^{2+} (quintet [Rn] $5f^4$), Th^+ (quartet [Rn] $6d^27s^1$), and Th^{2+} (triplet [Rn] $5f^16d^1$), an intersystem crossing takes place before the formation of that intermediate, and the corresponding $HMOH^{+(2+)}$ structures have triplet, doublet, and singlet spin ground states, respectively. The bare U^+ cation (quartet [Rn] $5f^37s^2$) has enough valence electrons available for bonding, so that the quartet spin state stays as the ground state all along the reaction pathway. The doublet spin is highly stabilized for all of the species involved in the path but never becomes the lowest-energy spin state.[5] The geometrical properties of the $HMOH^{+(2+)}$ species are very similar, with the only exception of $HUOH^{2+}$, which is linear and less stabilized with respect to the reactant asymptote.

Comparing the $Th^{+(2+)} + H_2O$ dehydrogenation reactions with the same reactions for U cations, we note the notably higher exothermicity in the case of Th cations, e.g. 379 and 366 kJ/mol for Th^+ and $Th^{2+} + H_2O$ (B3LYP/SDD), respectively, versus 208 and 127 kJ/mol of U^+ and $U^{2+} + H_2O$ reactions, respectively.[5] This result is not surprising considering the higher BDEs of the cationic thorium monoxides (Table 2) with respect to the corresponding uranium monoxides.[6]

In both cases, the intrinsic reaction barriers associated with the dipositive cations are higher than the corresponding barriers for the monocations (Table 4). Comparing the transition barriers of U^+ with respect to that of Th^+, we note that the main difference is found in the dissociation barrier, which is quite lower in the case of Th^+, because of the previously mentioned repulsive effects between the unpaired electron localized on the metal cation (s-type) and the H_2 molecule. In the case of the $(H_2)UO^+$ intermediate, the unpaired electrons are of f-type. The rest of the transition barrier heights can be considered comparable. The same comparison in the case of Th^{2+} and U^{2+} shows a clearer tendency that indicates higher barriers for U^{2+}. Experimental results have indicated a lowering of the reaction efficiency in going from Th^+ to U^+,[2] as well as from Th^{2+} to U^{2+}.[3]

The formation of the alternative product, $MOH^{+(2+)}$, is exothermic in all cases and, as previously remarked, in the case of thorium, the lowest-energy isomer does not always correspond to the structure having the hydroxyl connectivity. In our previous study[5] of the reaction of U cations with water, we have only reported the lowest-energy isomers, namely,

$UOH^+(^5A'')$ and UOH^{2+} ($^4A'$), but we have also studied singlet and triplet states in the case of the monocationic structure and the doublet and sextet spin states for the dicationic structure. We have also considered the possible formation of $HUO^{+(2+)}$ isomers; however, for U the hydroxyl connectivities are always preferred and the lowest-energy isomers are the previously mentioned $UOH^+(^5A'')$ and UOH^{2+} ($^4A'$).

4. Conclusions

The results of a theoretical study of the $Th^{+(2+)} + H_2O$ gas-phase reaction mechanisms were reported. According to our calculations, the dehydrogenation process is thermodynamically favored in both studied reactions. The formation of the alternative product, $ThOH^{+(2+)} + H$, was also found to be an exothermic process, in both reactions. We have found that the previously assumed hydroxyl connectivities do not always correspond to the lowest-energy isomers. In particular, in the case of the monopositive species, the lowest-energy structure has the oxide−hydride $HThO^+$ ($^1A'$) structure. That isomer could be formed from the lowest-energy $HThOH^+$ intermediate, only after the system surpasses an intrinsic barrier height of around 200 kJ/mol. In the dicationic reaction, the lowest-energy isomer, $ThOH^{2+}(^2A)$, could be formed directly from the excited-state $HThOH^{2+}$ intermediate, which is already prepared for the H detachment. For both reactions, all of the transition states are well below the dissociation limit represented by the reactants. The reaction barriers associated with dipositive cations are always higher than those corresponding to the monopositive case. From the present study and considering the large exothermicity of the studied reactions, it is not possible to get definitive conclusions that could explain the different branching ratios reported experimentally.

CCSD(T) single-point calculations were performed on the B3LYP/SDD-optimized geometries. All of the calculated barrier heights show a good agreement between the CCSD(T)//B3YLP and DFT calculations, with the only exception of the first TS1 transition barrier of the monocationic reaction, which involves two species having high T1 values and spin contamination problems. Calculations of T1 diagnostics indicate that three of the studied species are over the threshold of 0.02 (T1 = 0.033, 0.040, and 0.027, respectively) usually accepted to support the validity of a monodeterminantal description of the reference wave function. That indicates that the involved species present some degree of multireferencial character.

Acknowledgment. This research was founded by Università della Calabria.

Supporting Information Available: NBO and NPA analysis of all of the reaction products involved in both studied reaction pathways. This material is available free of charge via the Internet at http://pubs.acs.org.

IC701789N